J|A|C|S
COMMUNICATIONS

Published on Web 02/21/2007

Hexagonally Ordered Nanostructures Comprised of a Flexible Disk-like Molecule with High Self-Assembling Properties at Neutral and Cationic States

Masashi Hasegawa, Hideo Enozawa, Youhei Kawabata, and Masahiko Iyoda*

Department of Chemistry, Graduate School of Science and Engineering, Tokyo Metropolitan University, Hachioji, Tokyo 192-0397, Japan

Received December 17, 2006; E-mail: iyoda-masahiko@c.metro-u.ac.jp

Self-assembly of organic π-conjugated systems in solution can be widely utilized to construct unique, complex supramolecular structures.[1,2] Thus, π-conjugated molecules with either electron-withdrawing groups or large π-circles and disks self-aggregate in solution by $\pi-\pi$ stacking interactions and solvophobic effects.[3] On the other hand, solid state and surface organization of π-conjugated molecules is frequently applied to molecular electronics.[4,5] To control one-, two-, or three-dimensional arrangement of the molecule in the solid state, preaggregation of conjugated π-systems plays an important part.

Recently, TTF-containing oligomers, polymers, and dendrimers have been synthesized to investigate redox-active supramolecular structures.[6] In particular, conjugated TTF oligomers are regarded as candidates for building blocks of supramolecular systems because of their unique electronic properties at neutral, radical cationic, and polycationic states.[7] Quite recently, gelators having TTF moieties were reported to produce electroactive nanowires,[8,9] although all nanowires exhibit moderate to poor conductivities presumably due to the poor ability to form a good conduction path in the oxidized state. To take advantage of the stacking behavior of TTF as a driving force for constructing higher aggregates, hexakis(tetrathiafulvalenylethynyl)benzene (**1**) is an ideal molecule with a radial core (Chart 1). The present study deals with the synthesis of **1** and fabrication of hexagonal nanostructures using self-assembly of **1** and its cation radicals. The electric conductivities of cation radicals clearly reflect the difference of their nanostructures.

An efficient route to **1** was established by the Sonogashira coupling reaction of iodo-TTF **4** with hexaethynylbenzene **3** (Scheme 1). TTF hexamer **1** exhibits a purple color in chloroform solution with the longest absorption maximum at 559 nm. B3LYP/6-31G(d,p) calculations of **1** revealed that a disk-like C_6-conformation with a small torsional angle (dihedral angle between phenyl and TTF rings = 15°) is an energy minimum. In fact, the ^{1}H NMR spectrum of **1** (6.7×10^{-6} M) in $CDCl_3$ shows the TTF proton at low field (δ 6.96) due to the closely located S···H arrangement (SH is 3.156 Å based on calculation).[10]

Vapor pressure osmometric (VPO) measurements of **1** in chloroform revealed that neutral **1** self-associates to form aggregates higher than dimers, although reported 1,3,5-tris(tetrathiafulvalenylethynyl)benzene shows very weak association behavior in solution.[7a] Assuming an infinite association model, the association constant was determined with concentration dependence of electronic spectra in $CHCl_3$ ($K_a = 2.1 \times 10^4$ M^{-1} at 23 °C). Considering the fairly large K_a of **1**, association of **1** mainly depends on intermolecular attractive forces between terminal TTF groups based on weak S···S and $\pi-\pi$ interactions to form a columnar structure.

When a purple solution of **1** in $CHCl_3$ was cast on a glass surface, a blue film was formed. UV−vis spectrum of the film shows a red shift of the longest absorption maximum (600 nm). Interestingly, when hexane was added to a solution of **1** in $CHCl_3$, dark blue fibrous material with the longest wavelength absorption at 580 nm was formed. As shown in Figure 1A, a slender and frizzled wire structure (40−200 nm wide and 30−100 nm thick) more than 10 μm long was observed by the SEM and AFM measurement.[11]

Chart 1

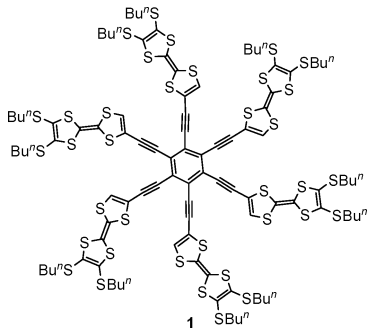

Scheme 1

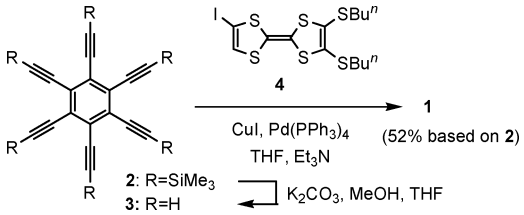

X-ray diffraction (XRD) studies on the film and fibrous material of **1** show that the two diffraction patterns are different. The diffractogram of the film showed a couple of reflections (d = 21.4 and 10.7 Å) with a broad reflection (d = 3.69 Å) corresponding to lateral order and $\pi-\pi$ stacking (Figure S15, Supporting Information),[12] whereas the diffractogram of the fibrous material exhibited a hexagonally ordered structure with a lattice constant a_0 = 32.1 Å (Figure 1B). Thus, an intense (100) reflection (d = 27.8 Å) with four weak higher-order reflections (d = 15.9 and 13.9 Å) allows the lattice to be indexed to a two-dimensional hexagonal arrangement. Furthermore, XRD experiments of powders prepared from the wires showed an additional reflection of d = 3.53 Å corresponding to a stacking structure (Figure S13, Supporting Information).

Oxidation of **1** measured by cyclic voltammetry in CH_2Cl_2 (1.5×10^{-5} M) shows a very broad wave of the first six-electron oxidation at −0.13 to 0.05 V (vs Fc/Fc$^+$) to form **1**$^{6+}$ and the second sharp six-electron oxidation wave at 0.32 V to form **1**$^{12+}$. The very broad oxidation wave for the formation of **1**$^{\bullet+}$−**1**$^{6+}$ reflects a complex aggregation of **1**, **1**$^{\bullet+}$, and **1**$^{n+}$ (n = 2−6) in solution. Analytically pure **1**$^{\bullet+}$·ClO_4^- and **1**$^{3+}$·$(ClO_4^-)_3$ can be prepared by chemical oxidation of **1** with $Fe(ClO_4)_3$. UV−vis−NIR spectra of the cation radicals in $CHCl_3$ show very broad NIR absorptions at ca. 2350 nm (log ϵ = 3.53) for **1**$^{\bullet+}$·ClO_4^- and ca. 2200 nm (log ϵ = 3.61) for **1**$^{3+}$·$(ClO_4^-)_3$ due to mixed valence state of a stacked

10.1021/ja069025+ CCC: $37.00

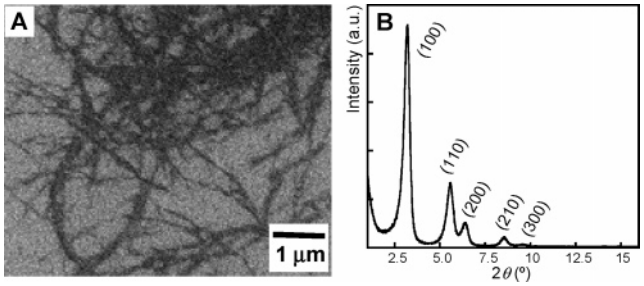

Figure 1. (A) SEM image of entangled fibrous material of neutral **1** with 5000× magnification. (B) XRD pattern of hexagonal nanowires of **1** on an aluminum plate.

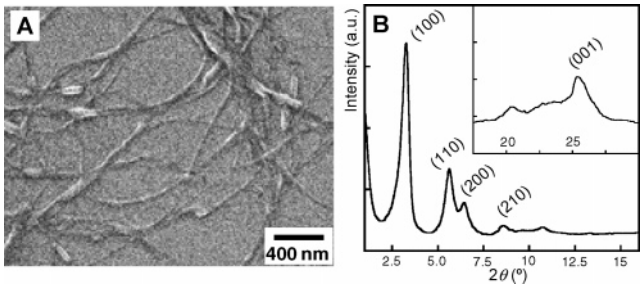

Figure 2. (A) SEM image of a fibrous material of $\mathbf{1}^{\bullet+}\cdot ClO_4^-$ with 5000× magnification. (B) Powder XRD patterns of a hexagonal columnar structure of $\mathbf{1}^{\bullet+}\cdot ClO_4^-$; the inset shows the region of $17.5 < 2\theta < 30°$.

$(TTF)_2^{\bullet+}$ unit, and the association constants of $\mathbf{1}^{\bullet+}\cdot ClO_4^-$ and $\mathbf{1}^{3+}\cdot(ClO_4^-)_3$ in $CHCl_3$ have been estimated to be $K_a = 2.3 \times 10^6$ and $2.5 \times 10^6\ M^{-1}$ (23 °C), respectively. Although a large cylinder structure of the stacked $\mathbf{1}^{\bullet+}$ and $\mathbf{1}^{3+}$ can be expected in solution,[13] ESR spectra of $\mathbf{1}^{\bullet+}\cdot ClO_4^-$ and $\mathbf{1}^{3+}\cdot ClO_4^-$ in $CHCl_3$ (23 °C) exhibit the existence of 100% spin for $\mathbf{1}^{\bullet+}$ ($g = 2.0068$) and 33% spin for $\mathbf{1}^{3+}$ ($g = 2.0073$), respectively, suggesting weak intermolecular spin−spin interaction in $\mathbf{1}^{\bullet+}$ and strong intramolecular spin−spin interaction in $\mathbf{1}^{3+}$.

Interestingly, deep green fibrous material was formed when a solution of $\mathbf{1}^{\bullet+}\cdot ClO_4^-$ in $CHCl_3$ was mixed with large amounts of hexane (Figure 2A). The nanowires are 40−80 nm wide and more than 20 μm long. In contrast, a deep green film was formed when a $CHCl_3$ solution of $\mathbf{1}^{\bullet+}\cdot ClO_4^-$ was cast on a glass surface. UV−vis−NIR spectra of the nanowires and film are very similar to that of $\mathbf{1}^{\bullet+}\cdot ClO_4^-$ in $CHCl_3$ presumably due to their multistacking structures. It is noteworthy that nanowires of $\mathbf{1}^{\bullet+}\cdot ClO_4^-$ (Figure 2A) seem to be loose probably due to Coulomb repulsion between the cationic charges, whereas nanowires of **1** (Figure 1A) prefer to gather to form an entangled structure.

XRD studies on the wires and drop-cast film of $\mathbf{1}^{\bullet+}\cdot ClO_4^-$ exhibit the remarkable structural differences, although their absorption and ESR spectra are very similar. The diffractograms of the wires of $\mathbf{1}^{\bullet+}\cdot ClO_4^-$ showed one intense ($d = 27.5$ Å) and four weak reflections based on a hexagonally ordered lamellar structure ($a_0 = 31.8$ Å) with the $\pi-\pi$ stacking distance of 3.51 Å (Figure 2B). In contrast, the diffractogram of the film of $\mathbf{1}^{\bullet+}\cdot ClO_4^-$ exhibited a couple of reflections ($d = 25.5$ and 13 Å) corresponding to laterally stacking arrangement. The longer distance ($d = 25.5$ Å) of the film of $\mathbf{1}^{\bullet+}\cdot ClO_4^-$ compared to that of **1** ($d = 21.4$ Å) may reflect more overlapping structure of $\mathbf{1}^{\bullet+}\cdot ClO_4^-$ which rises perpendicularly from the surface of the aluminum plate. Another point which should be noted is that the lattice constants (a_0) of nanowires of $\mathbf{1}^{\bullet+}\cdot ClO_4^-$ are smaller than that of **1** despite the presence of a ClO_4^- counteranion.

The electric conductivities of the wires and film of $\mathbf{1}^{\bullet+}\cdot ClO_4^-$ exhibit a considerable difference according to their different molecular arrangement. Thus, a small tape ($0.24 \times 0.10 \times 0.005$ mm) prepared from wires of $\mathbf{1}^{\bullet+}\cdot ClO_4^-$ showed a conductivity of $\sigma_{rt} = 1.1 \times 10^{-3}\ S\ cm^{-1}$, suggesting more effective conduction due to a hexagonally ordered columnar structure, whereas the film of $\mathbf{1}^{\bullet+}\cdot ClO_4^-$ showed a conductivity of $\sigma_{rt} = 3.1 \times 10^{-5}\ S\ cm^{-1}$.

In summary, we have synthesized a novel TTF hexamer **1** with a flexible disk-like structure, weak amphiphilic nature, and strong self-aggregation properties. Nanowires fabricated from **1** in a $CHCl_3$/hexane solution have a hexagonal columnar structure, reflecting the lateral and $\pi-\pi$ stacking interactions of its disk-like frame. Furthermore, we have also succeeded in formation of fibrous material with a hexagonal columnar structure from $\mathbf{1}^{\bullet+}\cdot ClO_4^-$. We believe this is a quite rare example of nanowires prepared from organic ion radical salts. The electric conductivity of the wire of $\mathbf{1}^{\bullet+}$ is 2 orders of magnitude higher than that of the film of $\mathbf{1}^{\bullet+}$, reflecting their nanostructured, one-dimensional morphologies.

Acknowledgment. This work was supported in part by a Grant-in-Aid for scientific research from JSPS. We would like to thank Prof. Y. Tobe (Osaka University) for his assistance with VPO measurements.

Supporting Information Available: Details of the synthesis, aggregation behavior, and characterization of nanostructures of **1**, $\mathbf{1}^{\bullet+}\cdot ClO_4^-$, and $\mathbf{1}^{3+}\cdot(ClO_4^-)_3$. This material is available free of charge via the Internet at http://pubs.acs.org.

References

(1) Höger, S. Shape-Persistent Acetylenic Macrocycles for Ordered Systems. In *Acetylenic Chemistry*; Diederich, F., Stang, P. J., Tykwinski, R. R., Eds.; Wiley-VCH: Weinheim, Germany, 2005.
(2) (a) Zhao, D.; Moore, J. S. *Chem. Commun.* **2003**, 807−818. (b) Yamaguchi, Y.; Yoshida, Z. *Chem.—Eur. J.* **2003**, *9*, 5430−5440. (c) Grave, C.; Schlüter, A. D. *Eur. J. Org. Chem.* **2002**, 3075−3098. (d) van Nostrum, C. F. *Adv. Mater.* **1996**, *8*, 1027−1030.
(3) Hoeben, F. J.; Jonkheijm, P.; Meijer, E. W.; Schenning, A. P. H. J. *Chem. Rev.* **2005**, *105*, 1491−1546.
(4) *Molecular Switches*; Feringa, B. L., Ed.; Wiley-VCH: Weinheim, Germany, 2001.
(5) *Molecular Devices and Machines*; Balzani, V., Venturi, M., Credi, A., Eds.; Wiley-VCH: Weinheim, Germany, 2003.
(6) (a) Iyoda, M.; Hasegawa, M.; Miyake, Y. *Chem. Rev.* **2004**, *104*, 5085−5113. (b) Segura, J. L.; Martín, N. *Angew. Chem., Int. Ed.* **2001**, *40*, 1372−1409. (c) Bryce, M. R. *J. Mater. Chem.* **2000**, *10*, 589−598. (d) Nielsen, M. B.; Lomholt, C.; Becher, J. *Chem. Soc. Rev.* **2000**, *29*, 153−164.
(7) (a) Hasegawa, M.; Takano, J.; Enozawa, H.; Kuwatani, Y.; Iyoda, M. *Tetrahedron Lett.* **2004**, *45*, 4109−4112. (b) González, A.; Segura, J. L.; Martín, N. *Tetrahedron Lett.* **2000**, *41*, 3083−3086.
(8) Gall, T. L.; Pearson, C.; Bryce, M. R.; Petty, M. C.; Dahlgaard, H.; Becher, J. *Eur. J. Org. Chem.* **2003**, 3562−3568.
(9) (a) Sly, J.; Kasák, P.; Gomar-Nadal, E.; Rovira, C.; Górriz, L.; Thorarson, P.; Amabilino, D. B.; Rowan, A. E.; Nolte, R. J. M. *Chem. Commun.* **2005**, 1255−1257. (b) Akutagawa, T.; Kakiuchi, K.; Hasegawa, T.; Noro, S.; Nakamura, T.; Hasegawa, H.; Mashiko, S.; Becher, J. *Angew. Chem., Int. Ed.* **2005**, *44*, 7283−7287. (c) Kitamura, T.; Nakaso, S.; Mizoshita, N.; Tochigi, Y.; Shimomura, T.; Moriyama, M.; Ito, K.; Kato, T. *J. Am. Chem. Soc.* **2005**, *127*, 14769−14775. (d) Kitahara, T.; Shirakawa, M.; Kawano, S.; Beginn, U.; Fujita, N.; Shinkai, S. *J. Am. Chem. Soc.* **2005**, *127*, 14980−14981. (e) Wang, C.; Zhang, D.; Zhu, D. *J. Am. Chem. Soc.* **2005**, *127*, 16372−16373.
(10) Iyoda, M.; Hasegawa, M.; Takano, J.; Hara, K.; Kuwatani, Y. *Chem. Lett.* **2002**, 590−591.
(11) Recent related examples: (a) Enozawa, H.; Hasegawa, M.; Takamatsu, D.; Fukui, K.; Iyoda, M. *Org. Lett.* **2006**, *8*, 1917−1920. (b) Balakrishnan, K.; Datar, A.; Zhang, W.; Yamg, X.; Naddo, T.; Huang, J.; Zuo, J.; Yen, M.; Moore, J. S.; Zang, L. *J. Am. Chem. Soc.* **2006**, *128*, 6576−6577. (c) Puigmartí-Luis, J.; Minoia, A.; del Pino, Á. P.; Ujaque, G.; Rovira, C.; Lledós, A.; Lazzaroni, R.; Amabilino, D. B. *Chem.—Eur. J.* **2006**, *12*, 9161−9175. (d) Nakao, K.; Nishimura, M.; Tamachi, T.; Kuwatani, Y.; Miyasaka, H.; Nishinaga, T.; Iyoda, M. *J. Am. Chem. Soc.* **2006**, *128*, 16740−16747.
(12) The film of **1** exhibits weak FET properties, reflecting a lamellar structure vertical to the substrate (Figure S16, Supporting Information).
(13) Small-angle X-ray scattering (SAXS) analysis of $\mathbf{1}^{\bullet+}$ and $\mathbf{1}^{3+}$ in THF reveals cylinder structures with 11 Å radius and 14−16 Å high, and hence three to five disk-like $\mathbf{1}^{\bullet+}$ and $\mathbf{1}^{3+}$ stacks on average, although **1** shows no self-aggregation in THF (Figure S24, Supporting Information).

JA069025+